

Introduction: Advances in surveying impact craters present in data gathered by remote sensing of planetary surfaces have not kept up with advances in data collection. As a result, there is a deluge of planetary data but no means for its comprehensive analysis. If left to manual surveys, the fraction of cataloged craters to the craters actually present in the available and forthcoming data will continue to drop precipitously. Therefore, we submit that automating the process of crater detection is the only practical solution to a comprehensive surveying of craters. As the first step to automating the surveying process we have developed [1,2] a robust crater detection algorithm (CDA) capable of identifying and characterizing most craters over the entire surface of Mars having diameter $D \geq 3$ km. The limit on the size of the crater is set by the resolution of topographic data used for crater detection. Presently, the global topographic coverage is given with the resolution of 1/128 degree by the MOLA Mission Experiment Gridded Data Record (MEGDR) [3].

Methods. Our CDA is a two stage system that first identifies round depression on Mars and then uses machine learning technique to separate true craters from false positives. Its application to the entire surface of Mars requires subdividing the surface into 356 overlapping tiles. The craters are identified and measured at each tile separately and the results from individual tiles are concatenated into a single catalog from which duplicate detections are eliminated. In its present “beta” version the catalog lists coordinates of the center of each crater, its diameter, depth, and an underlying geological unit.

Results. The catalog lists 75,919 craters ranging in size from 1.36 km to 347 km. Fig.1 shows the exceedance probability of crater diameter, D , for all craters in the catalog. Exceedance probability, $P(D > X)$, is a probability that a randomly chosen crater has diameter larger than X . It represent a convenient way of displaying distribution of crater sizes. For comparison, Fig. 1 also shows exceedance probability of crater diameter in manually collected Barlow [4] catalog that lists 42,283 craters. The graph reveals that the new catalog is statistically “complete” down to craters having size of about 3 km, whereas the Barlow catalog is statistically complete down to the size of 5 km. Fig. 2 shows that density of craters in the new catalog. The density is calculated using a moving circular window of radius 250 km. It reflects the combined effect of true distribution of craters and the existence of some

biases in the methodology due to different rate of automatic detection between different surfaces.

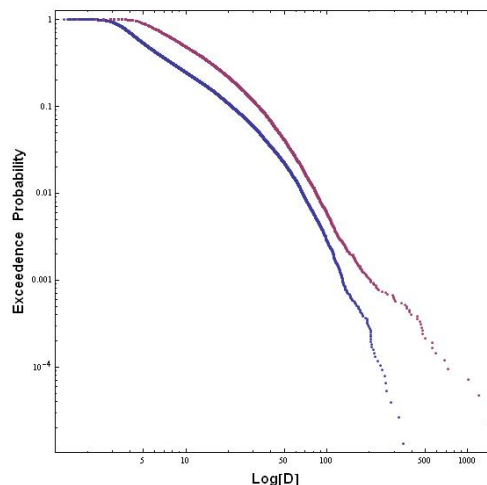


Figure 1: Exceedance probability of crater diameter D in the new catalog (blue) and the Barlow catalog (red). The curves level off at small values of D where few craters are present in the catalogs.

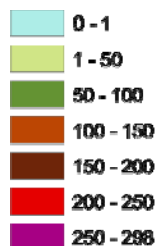
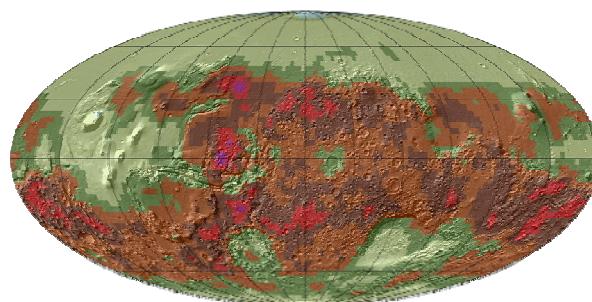


Figure 2: Crater density derived from the new catalog. Craters of all sizes are included. The numbers given in the legend are the number of craters in a circular window having radius of 250 km.

The new catalog can be used to map relative depths of craters over the entire Martian surface. For this purpose we have divided all craters into six size bins, $D < 5$ km (35,738 craters) , $5 \text{ km} \leq D < 10$ km (21,614

craters), $10 \text{ km} \leq D < 15 \text{ km}$ (6594 craters), $15 \text{ km} \leq D < 20 \text{ km}$ (3788 craters), $20 \text{ km} \leq D < 25 \text{ km}$ (2180 craters), $D \geq 25 \text{ km}$ (5971 craters). Using craters from each bin separately, maps of depth/diameter ratio (d/D) are constructed using moving average technique. Fig. 3 shows maps of (d/D) for bins 2, 4, and 6.

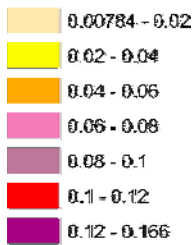
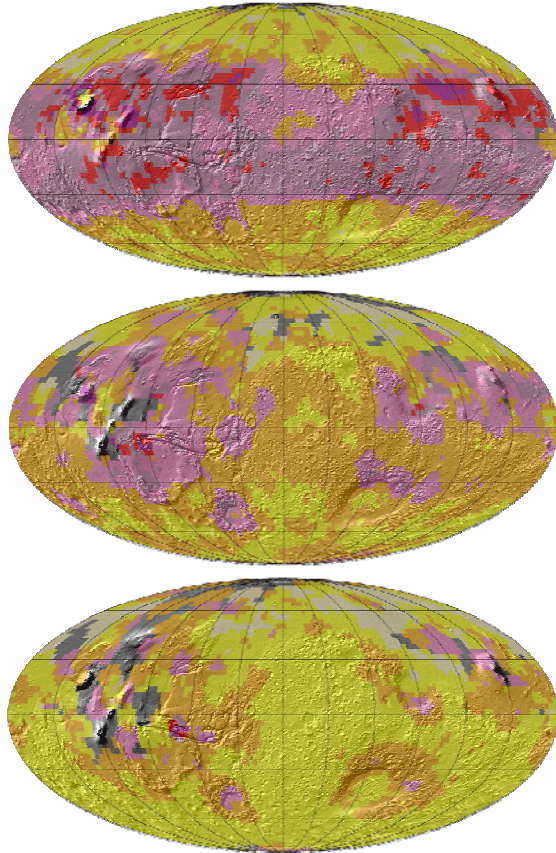


Figure 3: Global maps of spatial distribution of (d/D) on Mars. Maps of (d/D) constructed for craters $5 \text{ km} \leq D < 10 \text{ km}$ (top), $15 \text{ km} \leq D < 20 \text{ km}$ (middle), $D \geq 25 \text{ km}$ (bottom). Pixels that lacks sufficient number of craters in their neighborhood to calculate moving average are shown in gray.

Discussion: The maps reveal existence of different spatial patterns of (d/D) distribution. (1) For small craters with $D < 10 \text{ km}$ (the first two size bins) there is a clear latitudinal pattern. The Martian globe is divided into two zones, the equatorial zone ($Zone_E$, shown in reds) extending from the equator to the latitude of up to $\pm 40^\circ$, and the high latitude zone ($Zone_{HL}$, shown in

yellow) extending from to the latitude of $\sim \pm 40^\circ$ to the poles. In $Zone_E$ the craters are relatively deep, whereas in $Zone_{HL}$ the craters are relatively shallow. (2) For craters with $D > 25 \text{ km}$ (the sixth size bin) there is no obvious spatial pattern Throughout most parts of the globe the craters of these sizes have the same, low values of relative depths. (3) For $10 \text{ km} < D < 25 \text{ km}$ craters (the third to fifth size bins) some limited latitudinal dependence is observed and some regional dependence is also noticeable. The patterns on Fig. 3 can be explained by an existence of the cryosphere with the depth of its upper boundary significantly lowered in the equatorial regions, just as predicted by models based on ice stability concept [5,6,7]. Calculations [8,9,10] of viscous relaxation indicate that the style of crater modification depends on the depth of the cryosphere relative to the crater size. For a relatively deep cryosphere viscous relaxation leads to significant decrease of crater's (d/D) value. For a relatively shallow cryosphere there is no significant modification of crater's (d/D) value. In $Zone_E$ the high values of (d/D) for $D < 10 \text{ km}$ craters indicate absence of viscous relaxation and no cryosphere up to the depths of $\sim 1 \text{ km}$. In $Zone_{HL}$ the low values of (d/D) for $D < 10 \text{ km}$ craters indicate presence of viscous relaxation and cryosphere located just below the surface.

Overall, the new catalog serves two purposes. First, it demonstrates the feasibility of surveying craters by automatic means; further development will make possible surveys of sub-kilometer craters. Second, the new catalog makes possible the global map of craters depth. These maps need detailed studies to fully realize what they reveal.

References: [1] Stepinski, T. F. et al. (2007) *LPS XXXVIII*, Abstract #1338. [2] Stepinski, T.F. et al. (2007) *Icarus*, submitted. [3] Smith D. et al. (2003) NASA Planetary Data System, MSG-M-MOLA-5-MEGDR-L3-V1.0. [4] Barlow, N.G., (1988) *Icarus*, 75(2), pp. 285- 305. [5] Clifford S. M. and Hillel D. (1983) *JGR*, 88, 2456-2474. [6] Fanale F. P. et al. (1986) *Icarus*, 67, 1-18. [7] Clifford S. M. (1993) *JGR*, 98 E6, 10,973-11,016., 121-133. [8] Parmentier, E. M. and Head, J. W. (1981) *Icarus*, 47, 100-111. [9] Jankowski, D. G. and Squyers, S. W. (1993) *Icarus*, 106, 365-379. [10] Pathare, A. V. et al. (2005) *Icarus* 174, 396-418.